

# Synthesis and Structure of Mycolactone E Isolated from Frog *Mycobacterium*

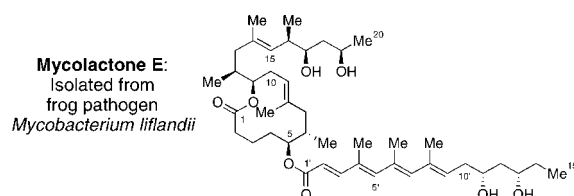
Sylvain Aubry,<sup>†</sup> Richard E. Lee,<sup>‡</sup> Engy A. Mahrous,<sup>‡</sup> Pam L. C. Small,<sup>§</sup> Dia Beachboard,<sup>§</sup> and Yoshito Kishi<sup>\*†</sup>

Department of Chemistry and Chemical Biology, Harvard University, 12 Oxford Street, Cambridge, Massachusetts 02138, Department of Pharmaceutical Sciences, University of Tennessee Health Science Center, 847 Monroe Avenue, Memphis Tennessee 38163, and Department of Microbiology, University of Tennessee, Knoxville, Tennessee 37996

kishi@chemistry.harvard.edu

Received September 25, 2008

## ABSTRACT



The structure of mycolactone E, isolated from the frog pathogen *Mycobacterium liflandii*, was established via organic synthesis. Within the mycolactone family of metabolites, a structural variation has been seen only at the unsaturated fatty acid moiety thus far, and mycolactone E follows this observation. Interestingly, the absolute configuration of its unsaturated fatty acid matches that of the mycolactones from human mycobacteria, rather than the structurally more closely related mycolactone F from fish mycobacteria.

Buruli ulcer is a severe necrotizing skin disease caused by *Mycobacterium ulcerans*, but it is one of the most neglected diseases.<sup>1</sup> Infection with *M. ulcerans*, probably carried by aquatic insects,<sup>2</sup> results in progressive necrotic lesions that, if untreated, can extend to 15% of a patient's skin surface. Currently, surgical intervention is the only realistic therapy.<sup>3</sup> In 1999, Small and co-workers isolated the toxic metabolites, named mycolactones A and B, from *M. ulcerans*. Evidence

from animal studies suggested that mycolactones A and B are directly responsible for the observed pathology.<sup>4</sup> The gross structure of mycolactones A and B was elucidated primarily through 2-D NMR experiments.<sup>5</sup> Their stereochemistry was predicted via the NMR database approach and then confirmed by total synthesis.<sup>6,7</sup> Through these studies, mycolactones A and B are now described as a mixture of *Z*- $\Delta^{4',5'}$ - and *E*- $\Delta^{4',5'}$ -geometric isomers (Scheme 1). Mycolactones A and B constitute the major metabolites produced

<sup>†</sup> Harvard University.

<sup>‡</sup> University of Tennessee Health Science Center.

<sup>§</sup> University of Tennessee.

(1) For general reviews on Buruli ulcer and mycolactones, see: (a) Asiedu, K.; Scherpier, R.; Raviglione, M., Eds. *Buruli ulcer: Mycobacterium ulcerans infection*; World Health Organization: Geneva, Switzerland, 2000. (b) Rohr, J. *Angew. Chem., Int. Ed.* **2000**, *39*, 2847. (c) Hong, H.; Demangel, C.; Pidot, S. J.; Leadlay, P. F.; Stinear, T. *Nat. Prod. Rep.* **2008**, *25*, 447.

(2) Marsollier, L.; Robert, R.; Aubry, J.; Saint Andre, J.-P.; Kouakou, H.; Legras, P.; Manceau, A.-L.; Mahaza, C.; Carbonnelle, B. *Appl. Environ. Microbiol.* **2002**, *68*, 4623.

(3) Fact Sheet Number 199, 2007, from World Health Organization (WHO) reports that treatment with rifampicin and streptomycin for eight weeks according to WHO guidelines leads to complete healing of nearly 50% Buruli lesions.

(4) George, K. M.; Chatterjee, D.; Gunawardana, G.; Welty, D.; Hayman, J.; Lee, R.; Small, P. L. C. *Science* **1999**, *283*, 854.

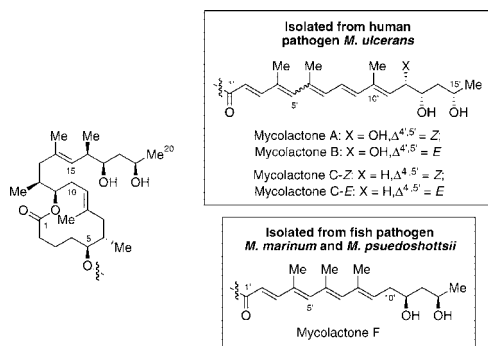
(5) Gunawardana, G.; Chatterjee, D.; George, K. M.; Brennan, P.; Whittorn, D.; Small, P. L. C. *J. Am. Chem. Soc.* **1999**, *121*, 6092.

(6) (a) Benowitz, A. B.; Fidanze, S.; Small, P. L. C.; Kishi, Y. *J. Am. Chem. Soc.* **2001**, *123*, 5128. (b) Fidanze, S.; Song, F.; Szlosek-Pinaud, M.; Small, P. L. C.; Kishi, Y. *J. Am. Chem. Soc.* **2001**, *123*, 10117.

(7) (a) Song, F.; Fidanze, S.; Benowitz, A. B.; Kishi, Y. *Org. Lett.* **2002**, *4*, 647. (b) Song, F.; Fidanze, S.; Benowitz, A. B.; Kishi, Y. *Tetrahedron* **2007**, *63*, 5739.

(8) (a) Mve-Obiang, A.; Lee, R. E.; Portaels, F.; Small, P. L. C. *Infect. Immun.* **2003**, *71*, 774. (b) Hong, H.; Gates, P. J.; Staunton, J.; Stinear, T.; Cole, S. T.; Leadlay, P. F.; Spencer, J. B. *Chem. Commun.* **2003**, 2822. (c) Hong, H.; Spencer, J. B.; Porter, J. L.; Leadlay, P. F.; Stinear, T. *ChemBioChem* **2005**, *6*, 643.

**Scheme 1.** Structures of the Mycolactones Isolated from Human and Fish Mycobacteria



by West African strains of *M. ulcerans*. However, several mycolactone congeners,<sup>1</sup> including mycolactone C,<sup>8</sup> were recently isolated from clinical isolates of *M. ulcerans* from Africa, Malaysia, Asia, Australia, and Mexico. With use of organic synthesis, the structure of mycolactone C was also elucidated (Scheme 1).<sup>9</sup>

Interestingly, a mycolactone-like metabolite, named mycolactone F, was isolated from the fish pathogen *M. marinum* as well as from *M. pseudoshottsii*,<sup>10</sup> and its complete structure was established with use of organic synthesis as the major tool.<sup>11</sup> Intriguingly, the absolute configuration of the 1,3-diol present in the unsaturated fatty acid of mycolactone F corresponds to the antipode of that present in the mycolactones isolated from the human mycobacteria.

A frog pathogenic mycobacterium was discovered and named *M. liflandii*.<sup>12</sup> Following importation of the West African clawed frog *Xenopus tropicalis*, a lethal frog disease, caused via infection of *M. liflandii*, appeared in the United States.<sup>12</sup> From lipid extracts, Small and co-workers succeeded in isolation of a partially purified mycolactone, called mycolactone E, and proposed the structure **II** (Scheme 2).<sup>13</sup> On the basis of MS analysis in combination with deuterium exchange and chemical transformation, Leadlay and co-workers suggested the alternative structure **I** (Scheme 2).<sup>14</sup> In this paper, we report a structure elucidation of mycolactone E with use of organic synthesis as the major tool.

Between the two proposed structures, the MS/MS fragmentation pattern, in particular, a fragment ion corresponding to  $[(M + Na) - 102 \text{ Da}]^+$  reported by Leadlay and co-workers,<sup>14</sup> supports **I** over **II**. For this reason, we chose first to focus on the proposed structure **I**. It is worthwhile to note that the gross structure difference between **I** and mycolactone F is only Mevs Et-group at the terminal position of unsaturated fatty acid.

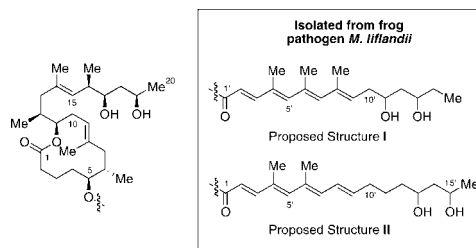
(9) Judd, T. C.; Bischoff, A.; Kishi, Y.; Adusumilli, S.; Small, P. L. C. *Org. Lett.* **2004**, *6*, 4901.

(10) (a) Ranger, B. S.; Mahrous, E. A.; Mosi, L.; Adusumilli, S.; Lee, R. E.; Colomi, A.; Rhodes, M.; Small, P. L. C. *Infect. Immun.* **2006**, *74*, 6037. (b) Hong, H.; Stinear, T.; Porter, J.; Demangel, C.; Leadlay, P. F. *ChemBioChem* **2007**, *8*, 2043.

(11) Kim, H.-J.; Kishi, Y. *J. Am. Chem. Soc.* **2008**, *130*, 1842.

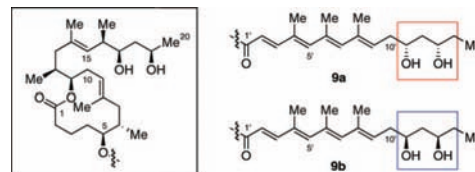
(12) Trott, K. A.; Stacy, B. A.; Lifland, B. D.; Diggs, H. E.; Harland, R. M.; Khokha, M. K.; Grammer, T. A.; Parker, J. M. *Comp. Med.* **2004**, *54*, 309.

**Scheme 2.** Proposed Structures for Mycolactone E Isolated from Frog Pathogen Mycobacterium



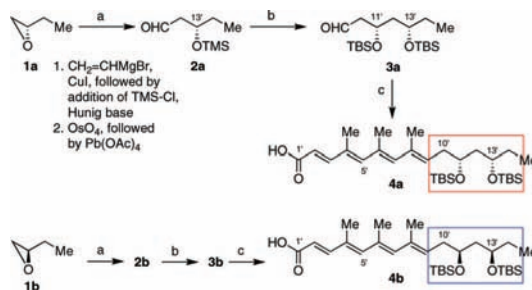
Therefore, we recognized the possibility that the complete structure of mycolactone E could be established via a direct extension of the strategy used for the case of mycolactone F. More specifically, we anticipated that two remote diastereomers **9a** and **9b** (Scheme 3) possible for **I** should play a central role

**Scheme 3.** Two Remote Diastereomers Possible for **I**



for this work and began the synthesis of **9a** and **9b** via the synthetic route used for mycolactone F.<sup>11</sup> Specifically, we first synthesized the unsaturated fatty acids **4a** and **4b** (Scheme 4)<sup>15</sup>

**Scheme 4.** Synthesis of Side-Chain<sup>a</sup>

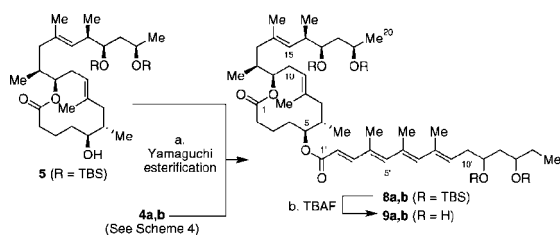


<sup>a</sup> Reagents and Conditions: (a) (1)  $\text{CH}_2=\text{CHMgBr}$ , CuI, THF, followed by addition of TMS-Cl, *i*-Pr<sub>2</sub>NEt. (2) OsO<sub>4</sub>, NMO, followed by Pb(OAc)<sub>4</sub> treatment; 67% overall yield. (b) Cr-mediated catalytic asymmetric allylation,<sup>15</sup> followed by: (1) aq HCl, (2) TBS-Cl, and (3) OsO<sub>4</sub>, NMO, then Pb(OAc)<sub>4</sub>. (c) Horner–Emmons olefination, followed by stepwise chain elongations consisting of DIBAL reduction, MnO<sub>2</sub> oxidation, and Horner–Emmons olefination. For the details, see Supporting Information and ref 11.

and then coupled **4a** and **4b** with the core alcohol **5**,<sup>7,16</sup> (Scheme 5), to furnish the two remote diastereomers **9a** and **9b**, respectively.

**Determination of Gross Structure.** Overall, we adopted the strategy precedent in the mycolactone F series. In the

### Scheme 5. Completion of Total Synthesis<sup>a</sup>



<sup>a</sup> Reagents and Conditions. Yamaguchi esterification: (a)  $\text{Cl}_3\text{C}_6\text{H}_2\text{COCl}$ , *i*- $\text{Pr}_2\text{NEt}$ , DMAP, PhH, rt, 24 h, 74%. (b) TBAF, THF, rt, 18 h, 76%.

mycolactone E series, however, we faced a new challenge: mycolactone E was available only in a very minute amount,<sup>17</sup> which presented a severe limitation in choosing an analytical method for comparison of the natural and synthetic materials. With this limitation, we first recorded the MS/MS spectra for the synthetic and natural materials under the identical conditions in a side-by-side manner. Although the relative peak intensity of  $[(M + \text{Na}) - 102 \text{ Da}]^+ / [M + \text{Na}]^+$  was found delicately to depend on each measurement, the synthetic material gave the MS/MS profile very similar to that of the natural mycolactone E.<sup>18</sup>

The MS/MS profile discussed supported the proposed gross structure **I**, but we wished to have more direct, unambiguous evidence to establish the gross structure. An obvious choice was to rely on the NMR spectroscopy, but the amount of natural mycolactone E available was unfortunately insufficient to measure a proton NMR spectrum.<sup>19</sup> Fortunately, however, an  $^1\text{H}$  NMR spectrum was recorded in one of our laboratories in 2005 (Figure 1).<sup>13,20</sup>

At first glance, we felt that the  $^1\text{H}$  NMR spectrum of natural mycolactone E was not consistent with the proposed gross structure **I**; more specifically, the  $\text{H}5'$  and  $\text{H}7'$  resonances stood out as a singlet at 6.43 and 6.05 ppm in the  $^1\text{H}$  NMR spectrum of **9a**, but no corresponding resonances were easily recognized in the  $^1\text{H}$  NMR spectrum of natural mycolactone E. However, on the basis of the knowledge gained in the mycolactone F series, we soon realized the possibility that this  $^1\text{H}$  NMR spectrum might not totally deny the proposed structure **I**.

As mentioned, the structural difference between mycolactone F and mycolactone E is minimal. Therefore, we anticipate the chemical behaviors of mycolactone E to be parallel with those observed on mycolactone F or its remote diastereomer. Although slow, we observed the geometric isomerism of mycolactone F under the standard laboratory

(13) Mve-Obiang, A.; Lee, R. E.; Umstot, E. S.; Trott, K. A.; Grammer, T. C.; Parker, J. M.; Ranger, B. S.; Grainger, R.; Mahrous, E. A.; Small, P. L. *C. Infect. Immun.* **2005**, *73*, 3307.

(14) Hong, H.; Stinear, T.; Skelton, P.; Spencer, J. B.; Leadlay, P. F. *Chem. Commun.* **2005**, 4306.

(15) For the Cr-mediate catalytic asymmetric allylation, see: Zhang, Z.; Aubry, S.; Kishi, Y. *Org. Lett.* **2008**, *10*, 3077.

(16) The core alcohol **5** was synthesized by Dr. Han-Je Kim in this laboratory.

(17) The lipid extract from fermentation broth of *M. liflandii* was used for this work. The amount of mycolactone E in this extract was estimated to be equivalent with ~10 injections for HPLC analysis.

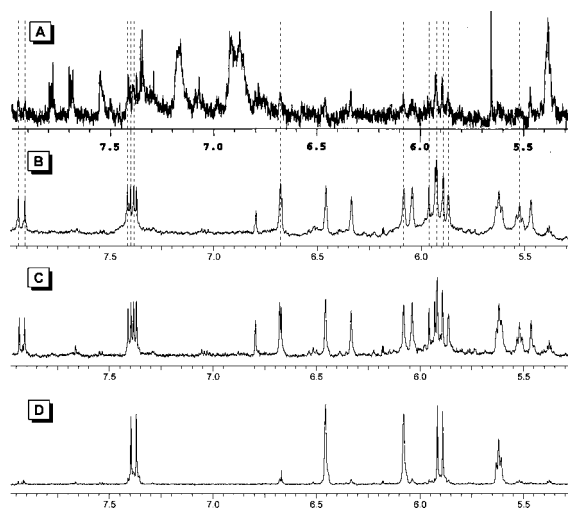


**Figure 1.**  $^1\text{H}$  NMR spectrum (acetone- $d_6$ ) of natural and synthetic mycolactone E. Panel A: natural mycolactone E (500 MHz). Panels D and C: before and after photochemical isomerization of synthetic mycolactone E **9a** (600 MHz). Panel B: after photochemical isomerization of **9a** (500 MHz). For the entire spectra shown in panels A–D and the corresponding spectra in the **9b** series, see Supporting Information.

conditions to yield a mixture of three predominant geometric isomers. Thus, an aged sample of mycolactone E should be composed of a mixture of the corresponding geometric isomers. Then, there is a possibility that the  $\text{H}5'$  and  $\text{H}7'$  protons might give six independent singlets, and therefore it could not be straightforward to detect these signals in the  $^1\text{H}$  NMR spectrum of natural mycolactone E.

To experimentally test this possibility, we subjected synthetic **9a** to a photochemically induced isomerization and obtained an approximately 1:1:1 mixture of the three dominant geometric isomers. With the use of the diagnostic chemical shifts identified in the mycolactone F series,<sup>11</sup> we assigned these products as all-*trans*-, *Z*- $\Delta^{4',5'}$ -, and *Z*- $\Delta^{6',7'}$ -geometric isomers (Scheme 6). The  $^1\text{H}$  NMR spectrum of the sample thus obtained is shown in Figure 1. Amazingly, all the signals present in this spectrum were detected in the  $^1\text{H}$  NMR spectrum of natural mycolactone E, thereby confirming the proposed gross structure **I**.

A parallel experiment was conducted on **9b**, a remote diastereomer of **9a**. As expected from our previous work,<sup>11,21</sup> **9b** exhibited the  $^1\text{H}$  NMR spectrum virtually identical to that of **9a**.<sup>18</sup> These experiments have now established that the structure of mycolactone E is represented by either **9a** or **9b**.

**Determination of Stereochemistry.** As before,<sup>11</sup> we relied on the chiral HPLC profile, to differentiate **9a** and its remote

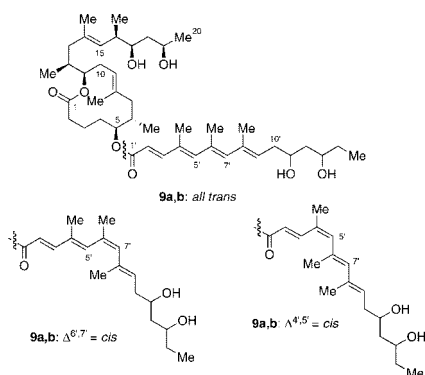
(18) See Supporting Information.

(19) Chronologically, we performed the HPLC comparison before the  $^1\text{H}$  NMR comparison (vide infra).

(20) To the best of our knowledge, this is the only  $^1\text{H}$  NMR spectrum ever recorded on natural mycolactone E.

(21) (a) Kobayashi, K.; Tan, C.-H.; Kishi, Y. *Helv. Chim. Acta* **2000**, *83*, 2562. (b) Boyle, C. D.; Harmange, J.-C.; Kishi, Y. *J. Am. Chem. Soc.* **1994**, *116*, 4995.

**Scheme 6. Photochemical Isomerism of 9a,b<sup>a</sup>**



<sup>a</sup> Photochemical isomerization was done in acetone with a Reonet photoreactor at 300 nm for 16 min, to furnish a 1:1:1 mixture of the three geometric isomers as the major products. The diagnostic chemical shifts (<sup>1</sup>H NMR in acetone-*d*<sub>6</sub>) are: 6.43 ppm (H-5') and 7.38 (H-3') for all-*trans* isomer; 6.66 (H-5') and 7.39 (H-3') for *Z*- $\Delta^{6,7}$  isomer; **5c**: 6.32 (H-5') and 7.93 (H-3') for *Z*- $\Delta^{4,5}$  isomer.<sup>11</sup> For the time-course of photochemistry, see Supporting Information.

diastereomer **9b**. For the HPLC experiments, we purposely used the photochemically equilibrated mixture of **9a** and **9b**, with the hope that each of their geometric isomers should give a distinct retention time, and therefore the HPLC comparison could be performed on the basis of six, instead of two, distinct retention times. Experimentally, we found that a Chiralpak IA chiral column in a mixture of benzene and ethanol meets our need well; with a fine-tuning on the ratio of two solvents, all of the six remote diastereomers, i.e., all-*trans*-, *Z*- $\Delta^{4,5}$ -, and *Z*- $\Delta^{6,7}$ -isomers of both **9a** and **9b**, gave a distinct retention time (Figure 2).<sup>22</sup> We then applied this HPLC condition to natural mycolactone E (Figure 2, panel a), thereby showing that natural mycolactone E and the 1:1:1 mixture of three geometric isomers of **9a** exhibit the identical HPLC profile. This conclusion was further confirmed via a coinjection of the natural and synthetic materials (Figure 2, panels b and c). These experiments have established that the natural product used for the comparison is a mixture of the three major geometric isomers of **9a**, but not **9b**. At present, we have not established whether the intact natural product is a single geometric isomer or a mixture of the three geometric isomers.

In conclusion, we have established the complete structure of mycolactone E isolated from the frog pathogen *M. liflandii* in a stepwise manner. First, the proposed gross structure **I** was confirmed via (1) the synthesis of **9a** and its remote diastereomer **9b**, (2) the photochemical isomerization of **9a** and **9b** into a 1:1:1 mixture of the three major geometric isomers, and (3) the <sup>1</sup>H NMR comparison of these mixtures with that of natural mycolactone E, recorded in 2005. Second,

(22) For the mycolactone F case, a mixture of isopropanol and toluene was used as an eluting solvent. The HPLC profile in two solvent systems is significantly different. For the details, see Supporting Information.

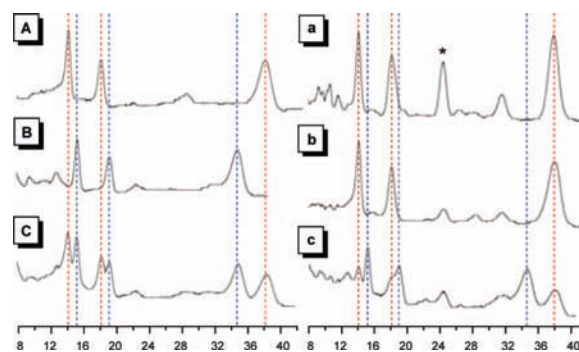


**Figure 2.** HPLC analysis of synthetic photochemically isomerized mycolactone E (**9a**), its remote diastereomer **9b**, and natural mycolactone E.<sup>22</sup> Column, Chiral Tech, Chiralpak IA (5  $\mu$ m), 250  $\times$  4.6 mm; Solvent (isocratic), EtOH/PhH = 1.5/98.5; flow rate, 1 mL/min; detection, absorption at 323 nm. Panel A: **9a**. Panel B: **9b**. Panel C: an ca. 1:1 mixture of **9a** and **9b**. Panel a: the lipid extract containing natural mycolactone E.<sup>17</sup> Peak indicated by \* corresponds to the C13'-ketone. Panel b: an ca. 1:1 mixture of mycolactone E and synthetic **9a**. Panel c: an ca. 1:1 mixture of natural mycolactone E and synthetic **9b**.

the stereochemistry was deduced via (1) the establishment of an HPLC analytical method to differentiate **9a** from **9b**, and (2) the established analytical method was applied to the natural product, thereby establishing the complete structure of mycolactone E as **9a**. Within mycolactones isolated from the *human* and *fish* mycobacteria, a structural variation has been seen only at the unsaturated fatty acid moiety thus far, and mycolactone E isolated from the *frog* mycobacterium follows this observation. Interestingly, the absolute configuration of its unsaturated fatty acid matches that of the mycolactones from the human mycobacteria, rather than the structurally more closely related mycolactone from the fish mycobacteria. Lastly, we should note that the supply of structurally well-defined mycolactone E and its remote diastereomer for biological tests is now secured via organic synthesis.

**Acknowledgment.** We thank Dr. Han-Je Kim in one of our laboratories for valuable discussion. We thank Drs. Phil Saxton and Nancy Wong at Eisai Research Institute for performing MS experiments. We are grateful to the National Institutes of Health (YK: CA 22215; PS: R01-1015-084) and to the Eisai Research Institute (Y.K.) for generous financial support. S.A. gratefully acknowledges a postdoctoral fellowship from Association pour la Recherche sur le Cancer (A.R.C.).

**Supporting Information Available:** Experimental details and <sup>1</sup>H and <sup>13</sup>C NMR spectra of key compounds. This material is available free of charge via the Internet at <http://pubs.acs.org>.

OL802233F